



ASME Accepted Manuscript Repository

Institutional Repository Cover Sheet

Carlos

Ledezma

*First*

*Last*

ASME Paper Title: Bridging Organ- and Cellular-Level Behavior in Ex Vivo Experimental Platforms Using Populations of Models of Cardiac Electrophysiology

Authors: Carlos A. Ledezma, Benjamin Kappler, Veronique Meijborg, Bas Boukens, Marco Stijnen, P. J. Tan and Vanessa Díaz-Zuccarini

ASME Journal Title: Journal of Engineering and Science in Medical Diagnostics and Therapy

Volume/Issue Volume 1 Issue 4

Date of Publication (VOR\* Online) July 24, 2018

ASME Digital Collection URL: <http://medicaldiagnostics.asmedigitalcollection.asme.org/article.aspx?articleid=26865>

DOI: 10.1115/1.4040589

\*VOR (version of record)

**Carlos A. Ledezma**

Department of Mechanical Engineering,  
University College London,  
London WC1E7JE, UK

**Benjamin Kappler**

LifeTec Group,  
Eindhoven 5611 ZS, The Netherlands

**Veronique Meijborg**

Department of Medical Biology,  
Amsterdam UMC,  
Amsterdam 1105 AZ, The Netherlands

**Bas Boukens**

Department of Medical Biology,  
Amsterdam UMC,  
Amsterdam 1105 AZ, The Netherlands

**Marco Stijnen**

LifeTec Group,  
Eindhoven 5611 ZS, The Netherlands

**P. J. Tan**

Department of Mechanical Engineering,  
University College London,  
London WC1E7JE, UK

**Vanessa Díaz-Zuccarini<sup>1</sup>**

Department of Mechanical Engineering,  
University College London,  
London WC1E7JE, UK  
e-mail: v.diaz@ucl.ac.uk

# Bridging Organ- and Cellular-Level Behavior in Ex Vivo Experimental Platforms Using Populations of Models of Cardiac Electrophysiology

*The inability to discern between pathology and physiological variability is a key issue in cardiac electrophysiology since this prevents the use of minimally invasive acquisitions to predict early pathological behavior. The goal of this work is to demonstrate how experimentally calibrated populations of models (ePoM) may be employed to inform which cellular-level pathologies are responsible for abnormalities observed in organ-level acquisitions while accounting for intersubject variability; this will be done through an exemplary computational and experimental approach. Unipolar epicardial electrograms (EGM) were acquired during an ex vivo porcine heart experiment. A population of the Ten Tusscher 2006 model was calibrated to activation–recovery intervals (ARI), measured from the electrograms, at three representative times. The distributions of the parameters from the resulting calibrated populations were compared to reveal statistically significant pathological variations. Activation–recovery interval reduction was observed in the experiments, and the comparison of the calibrated populations of models suggested a reduced L-type calcium conductance and a high extra-cellular potassium concentration as the most probable causes for the abnormal electrograms. This behavior was consistent with a reduction in the cardiac output (CO) and was confirmed by other experimental measurements. A proof of concept method to infer cellular pathologies by means of organ-level acquisitions is presented, allowing for an earlier detection of pathology than would be possible with current methods. This novel method that uses mathematical models as a tool for formulating hypotheses regarding the cellular causes of observed organ-level behaviors, while accounting for physiological variability has been unexplored. [DOI: 10.1115/1.4040589]*

## 1 Introduction

Ex vivo beating heart experiments allow a porcine heart to be investigated under working conditions that are closer to those found in vivo when compared to other ex vivo preparations, like Langendorff [1]. Namely, the heart perfuses the coronary system itself, the blood flows in the natural direction, the heart regains sinus rhythm, and adjustable pre- and after-load containers mimic the systemic and pulmonary circulations [2]. Consequently, these experiments, like the PhysioHeart platform [1] (LifeTec Group, Eindhoven, The Netherlands), have been used as a model to test medical devices destined to treat heart failure [2,3]. Given their resemblance to in vivo physiology, ex vivo beating heart platforms have the potential to become benchmarks for early stage drug trials (e.g., cardiotoxicity). However, there are still unknown physiological processes that cause the hearts to fail during the experiments; these usually end with an abrupt drop in cardiac output (CO), an inability of the heart to perfuse its own coronary system, and a loss of myocardial contractility. The time at which this end point is reached is, at the moment, unpredictable because it varies depending on the condition of the heart upon arrival to the laboratory and on the experimental protocol. Understanding the causes for the drop in cardiac performance is essential if these platforms will be used for translational work. Consequently, novel monitoring techniques are required to assess the physiology of the

porcine hearts during the working mode; these novel monitoring methods would enable the design of feedback protocols that would delay the end point and enhance reproducibility and clinical translatability. Additionally, understanding the causes for heart failure during the experiments would also provide insight on the onset and evolution of this disease.

The hypothesis explored in this work is that the analysis of individual cell biomarkers, and in particular electrophysiological features, could signal high risk of pathology at an early stage within these experiments. Then, it would be possible to intervene in the platform and solve the issue that would cause the heart to fail. The main challenge is that, because of experimental limitations, beating heart platforms preclude the use of cellular explorations like optocardiography [4] or monophasic action potential (AP) mapping, so less invasive acquisitions and surrogate measurements for action potential features must be implemented. However, a limitation of a surrogate approach is the need to establish whether the observations are a signature of pathological behavior or a manifestation of the normal physiological variation known as inter or intrasubject variability. This paper addresses these limitations with a combined experimental and computational approach.

The understanding of how cardiomyocytes behave has immensely benefited from electrophysiology mathematical models, which allow researchers to explore questions that would be impossible to test on human subjects or in ex vivo experiments because of technological limitations. In silico approaches, such as the pseudo-ECG [5] and the in silico ischemia [6] studies, have been employed to simulate physiology and pathology in order to elucidate how cellular processes and behavior affect organ acquisitions. The inverse

<sup>1</sup>Corresponding author.

Manuscript received May 16, 2018; final manuscript received June 11, 2018; published online July 24, 2018. Editor: Ahmed Al-Jumaily.

problem, however, is much more complicated since it is both ill-posed and highly sensitive to intersubject variability [7]. An additional complication is that models for cardiac electrophysiology are based mainly on averaged responses which represent the most common case; a consequential limitation is that, in their existing form, model predictions cannot discriminate pathological behavior from normal physiological variability [8]. Notwithstanding, “experimentally calibrated populations of models” (ePoM) [9–12] is a promising recent development that includes the effects of variability in the model parameters. However, statistical tools are still needed to interpret the myriad of action potential trajectories contained within a population of models in order to ascertain whether a particular biomarker is representative of a diseased state.

The main goal of this paper is to present a proof of concept for a novel technique on the application of mathematical models, through the statistical treatment of ePoMs, to elucidate the cellular causes for pathological behaviors observed in organ-scale acquisitions and to understand the role of variability in the detection of pathology. The method is useful when analyzing experimental data, because it produces cellular-level information that would be impossible to acquire without compromising the clinical translatability of the experiment. This proof of concept was applied, as an exemplary case, to deduce the cellular origins to CO reduction observed in a PhysioHeart experiment.

## 2 Materials and Methods

**2.1 Experimental Acquisitions.** The data reported in this paper were acquired during one PhysioHeart LifeTec Group, (Eindhoven, The Netherlands) experiment where the porcine heart was paced at 600 ms intervals. During the experiment, pressures, flows, and blood samples were assessed as routinely done in PhysioHeart experiments [1,2]. In the present study, it was hypothesized that an analysis of the electrical activity of the heart could provide a better understanding of the evolution of pathologies within the heart itself when compared to the aforementioned acquisitions, in particular through the application of populations of cardiac electrophysiology models as a means to elucidate the cellular causes for the observed pathological behavior. To test this hypothesis, left ventricular unipolar epicardial electrograms (EGM) were acquired by means of a custom-made square grid of 121 electrodes. Recordings were made, simultaneously, by all electrodes at three time points: 90 (time point 1, baseline), 120 (time point 2, midpoint), and 150 (time point 2, end point) min into the start of the working mode.

The porcine heart reported in this paper was harvested from a pig slaughtered for human consumption by personnel from the abattoir. Immediately after the animal was slaughtered the heart was harvested, after which the animal was closed again to continue the normal slaughterhouse process. The protocols for the harvest were developed in accordance with EC regulation 1774/2002, as supervised by the Dutch Ministry of Agriculture, Nature and Food Quality, and approved by the Food and Consumer Product Safety Authority. The harvesting of the heart was overseen by a veterinarian from the Dutch Food and Consumer Safety Department, thus ensuring that the animal was still suitable for human consumption afterwards. The inclusion criteria for the pigs and the full harvesting process were described in previous works [1]. Ethics approval for the study protocol was not required by the authors’ institutional guidelines and national laws and regulations.

**2.2 Population of Models.** The Ten Tusscher and Panfilov 2006 model (TP06) for ventricular myocytes [13,14] is adopted here to simulate the electrical behavior of the cardiac cells. In short, each equation in the model emulates a mechanism through which the cardiac myocyte absorbs or releases a given ion and the parameter of each equation controls the expression of that mechanism. For instance, the equation for  $I_{Na}$  has been designed to reproduce the initial fast sodium intake that produces the fast depolarization of the cell and the parameter  $G_{Na}$  regulates the

maximum amplitude of  $I_{Na}$ ; consequently, an elevated  $G_{Na}$  will produce a larger and faster initial upstroke in the action potential and as  $G_{Na}$  approaches zero the initial depolarization phase will disappear. A thorough description about the physiological meaning of all the model’s equations and parameters can be consulted in the original research paper [14]. The TP06 provides a mathematical description of the main ionic currents that are involved in AP genesis and has been thoroughly validated in the literature; for this reason, the TP06 model remains widely used for a variety of novel applications [6,15,16] including population-based studies [17]. A full discussion about the use, validity, and limitations of the TP06 for this study will be described later on.

The general contention in every study involving populations of cardiac electrophysiology models is that action potential variability is a consequence of changes in the magnitude of the ionic currents that produce the AP, as opposed to a change in their underlying dynamics [8]. Therefore, a population of models (PoM) was generated here by varying all the peak conductances and maximal currents in the TP06 model, these parameters are listed in the literature [14]. The space of parameters available to produce variations of the TP06 model is generated by multiplying the normal value of each parameter by  $N$  linearly spaced factors  $k_i$  ( $i \in [1, N]$ ), of between 0 and 2, given by

$$k_i = i * 2 / N \quad (1)$$

The use of these multiplying factors has previously been shown to capture both reduction and over-expression of the model parameters [12].

The parameter sampling space takes the form

$$\begin{pmatrix} k_1 G_{Na} & k_1 G_{to} & \dots & k_1 G_{bCa} \\ k_2 G_{Na} & k_2 G_{to} & \dots & k_2 G_{bCa} \\ \vdots & \vdots & & \vdots \\ k_N G_{Na} & k_N G_{to} & \dots & k_N G_{bCa} \end{pmatrix} \quad (2)$$

from which one model is generated by selecting a value from each column and solving the TP06 equations with the selected parameters. Models were obtained from the sampling space using Latin hypercube sampling (LHS), a method that ensures that all the values from the parameter space are represented [18]. Consistent with previous PoM studies [19], a total of  $N = 15,000$  samples were selected to construct the population of models. Models were solved with 600 ms cycle length and the PoM was the collection of the steady-state responses of the models selected by LHS. Models that produced physiologically impossible responses were excluded from the PoM by the following criteria: (1) action potential duration (APD90)  $\notin [100, 400]$  ms, (2)  $V_{max} < 0$ , (3)  $V_{rest} > -64$  mV, (4) upstroke time exceeding 10 ms.

**2.3 Calibration of the Population of Models.** Activation–recovery intervals (ARI) were measured from the EGMs through custom-made computer routines as suggested by Coronel et al. [20]. Namely, the activation time was measured as the time instant when the derivative of the EGM was minimal during the QRS complex and the recovery time as the time instant when the derivative was maximal during the  $T$  wave. Then, the ARI was the time difference between the activation and recovery moments. The ARI measurement is exemplified, for a single beat, in Fig. 1. Haws and Lux [21] and Potse et al. [22] have previously shown that the ARI is an adequate surrogate measurement for action potential duration at 90% repolarization (APD90). Hence, it can be argued that a model from the PoM reproduces the physiology of the myocytes observed in the experiment if its APD90 is similar to the ARI measured from the EGMs.

The process of finding all the models from the PoM that correspond to a given ARI is called “experimental calibration,” and the population that contains all these models is called ePoM. In this study, the PoM was calibrated to each channel, at each time point,

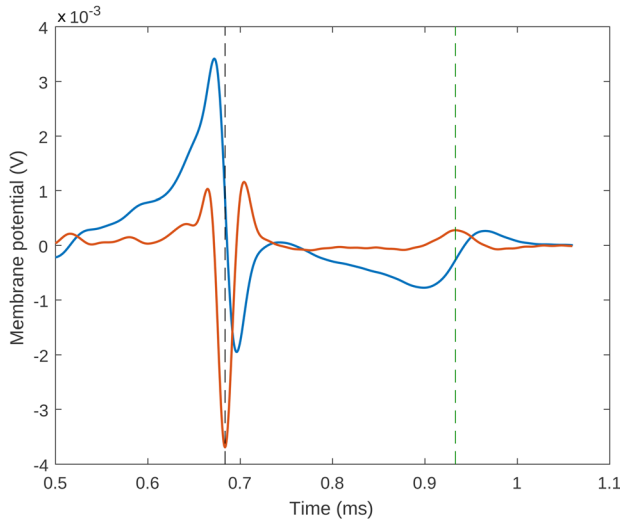


**Fig. 1** Example of ARI measurement. The image shows a typical beat (positive deflection), its derivative (negative deflection, scaled for clarity), its activation time (vertical line on the left), and recovery time (vertical line on the right).

by selecting all the models from the PoM that had APD90 in the range  $\mu_{ARI} \pm \sigma_{ARI}$  of that channel, at that time point. Here,  $\mu_{ARI}$  was the mean value of the ARIs measured at a given channel and time point, and  $\sigma_{ARI}$  their standard deviation. An example of the calibration process can be observed in Fig. 2.

Then, each channel, at each time point, was represented by a collection of models (an ePoM) that were, *potentially*, representative of the behavior observed in the EGM. Each ePoM is characterized by the statistical distribution of the parameters of the models contained within it. The distribution of a given parameter from a “healthy” ePoM and that of the same parameter from a “pathological” ePoM were compared by means of a Mann–Whitney–Wilcoxon (MWW) *U*-Test [23]. Then, if there was a statistically significant difference ( $\rho \leq 0.001$ ), the parameter responsible for the pathology was identified. ePoMs were only compared between those calibrated to the same channel at different times of the experiment; this was to identify spatial differences.

The process described in this section may be summarized by the flowchart presented in Fig. 3, where one can observe how the different methods previously explained come together in a single algorithm for the analysis of experimental data through populations of models. The diagram begins with the use of the TP06 model to generate a PoM; the parameters to be used are selected from the space of possible parameters using LHS. The resulting population is then calibrated to ARI measured from experimentally acquired left-ventricular EGM; this results in an ePoM per channel, per time

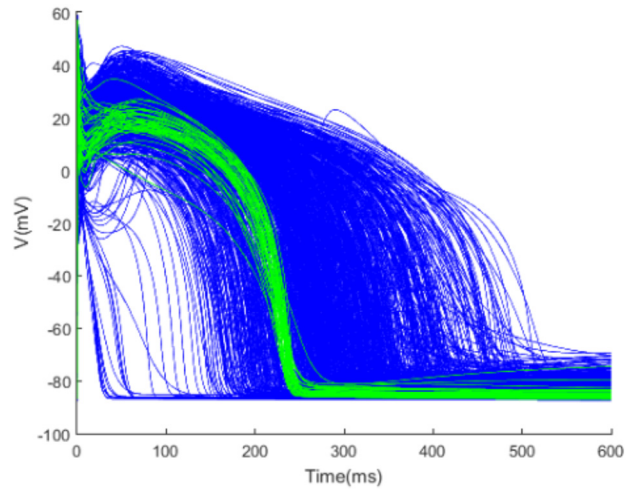


**Fig. 2** Example of experimental calibration. The figure shows the full population of TP06 models and, highlighted, the ePoM corresponding to ARIs in the range [220,250] ms.

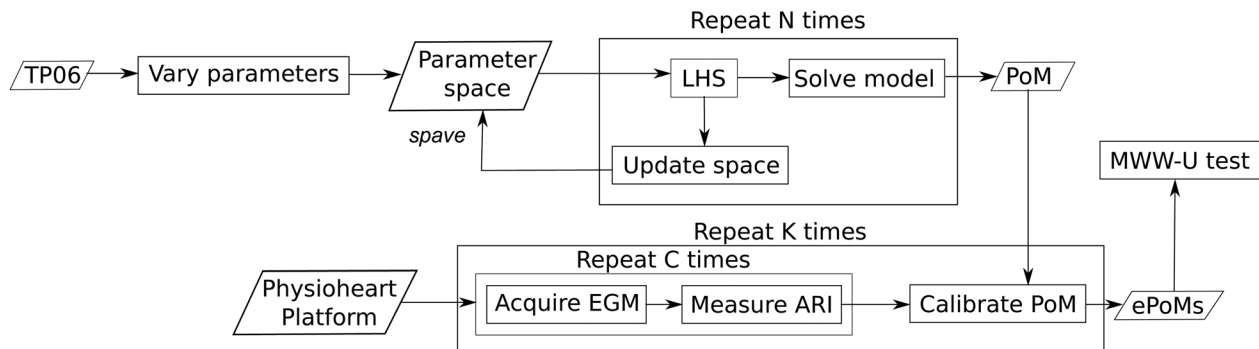
point. The ePoMs calibrated at different time instants, on the same channel, are compared using a MWW-*U* test.

### 3 Results

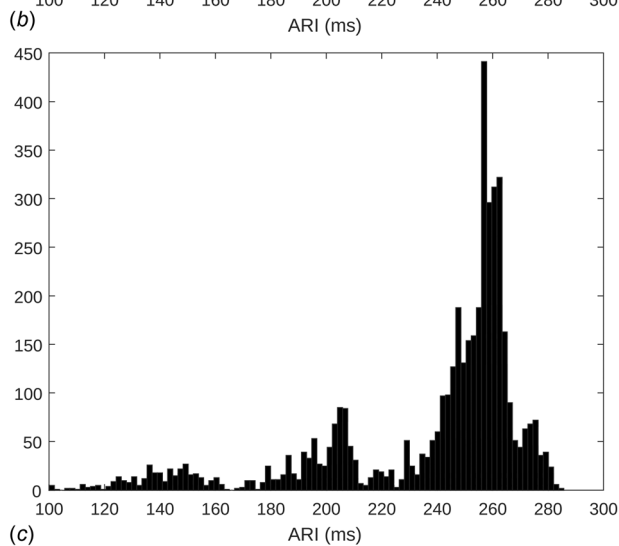
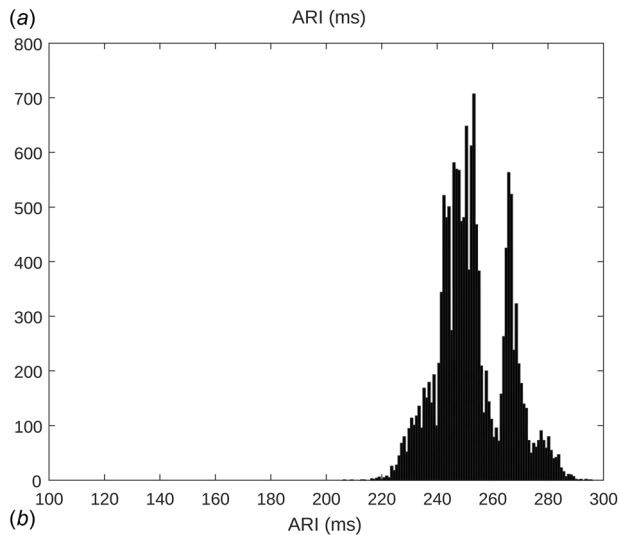
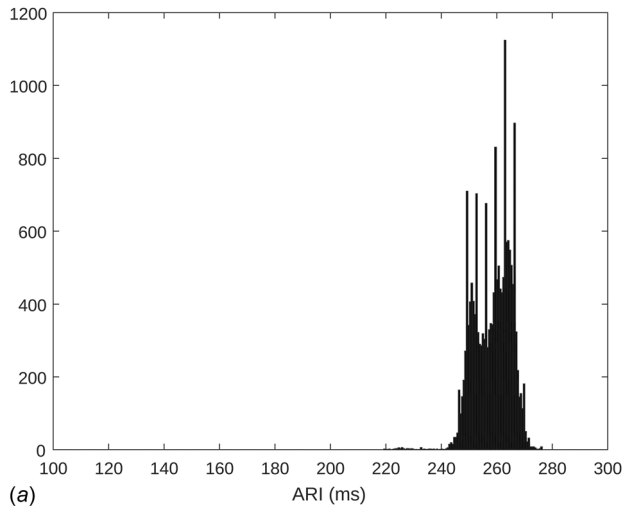
The mean CO was 3.8 L/min in average at the beginning of the acquisitions (90 min into the start of the working mode) and remained stable until the second time point (30 min later). Nevertheless, there was a noticeable decrease in CO, to 2.6 L/min, when the third measurement was taken (30 min after the second measurement), signaling the end point of the experiment.

Figure 4 shows the histograms of all the ARIs measured at each time point on the whole grid. Figure 4(a) shows the ARIs clustered around 260 ms and with less than 20 ms (7%) deviation in the first acquisition. Assuming that the activation is fast and homogeneous, this is the expected physiological behavior. This result, together with the CO at this time, supported the choice of this time point as the healthy benchmark to which the subsequent acquisitions were compared. In Fig. 4(b), one can observe ARIs below 240 ms and in Fig. 4(c) ARIs with values as low as 100 ms were recorded. It is this pathological reduction in ARI that was investigated through the comparison of the ePoMs.

The main results of the statistical analysis are tabulated in Table 1, which gives the number of channels that showed a statistically significant difference, with respect to the baseline measurement, for each of the parameters. The main highlight is that over half of the channels showed a significant difference in the L-type calcium conductance at time point 2, and this number increased above two-thirds at time point 3.



**Fig. 3** Flowchart summarizing the proposed methodology. Here,  $N = 15,000$  samples to be taken using LHS,  $K = 3$  time points at which the experimental acquisitions were made and  $C = 121$  electrodes in the grid.



**Fig. 4** Histograms showing the distribution of ARIs at the three time points of the experiment: (a) time point 1, (b) time point 2, and (c) time point 3

Figure 5 shows the boxplots of the parameter distributions of the three ePoMs, one for each time point, for a representative channel. It shows that the median value of  $G_{CaL}$  decreased dramatically as the experiment progressed in time. Also, the main repolarizing potassium-related conductances (i.e.,  $G_{Ks}$ ,  $G_{Kr}$ , and  $G_{Kl}$ ) were above their standard value from the beginning of the experiment. Given the above, the statistical analysis points toward

**Table 1** Number of channels showing a statistically significant difference, with respect to the baseline measurement, in the parameters of their ePoM

| Parameter  | Comparing 1–2 | Comparing 1–3 |
|------------|---------------|---------------|
| $G_{Na}$   | 0             | 0             |
| $G_{to}$   | 0             | 1             |
| $G_{Ks}$   | 6             | 11            |
| $G_{Kr}$   | 11            | 14            |
| $G_{Kl}$   | 0             | 0             |
| $P_{NaK}$  | 2             | 2             |
| $G_{CaL}$  | 61            | 85            |
| $k_{NaCa}$ | 0             | 0             |
| $G_{pCa}$  | 3             | 5             |
| $G_{pK}$   | 0             | 0             |
| $G_{bNa}$  | 0             | 0             |
| $G_{bCa}$  | 0             | 0             |

a generalized blockage in calcium uptake through L-type channels and elevated, but unchanging, potassium conductances as the most likely causes for the reduction in ARI.

Finally, the analyses from the blood samples, taken one at each time point, revealed increasing calcium and sodium concentrations as the experiment progressed and a high, but constant, potassium concentration throughout the working mode.

## 4 Discussion

**4.1 Suitability of the TP06 for This Study.** It is important to highlight that this paper focuses on the development of a proof of concept and novel methodological approach to underpin cellular behaviors that are responsible for observations made in organ-level acquisitions. Although TP06 is a model for human ventricular myocytes, it is our contention that in this light, its use to model the electrical activity of swine myocytes is appropriate. Various studies have shown that pigs have heart rates, hemodynamics, electrocardiographic and electrophysiological parameters that are comparable, and closer than any nonprimate animal, to humans [24–26]. The interspecies differences in ion current magnitudes were accounted for in the generation of the PoM; this is because a change in a peak current or maximal conductance parameter will produce an equivalent change in the current magnitude. It is also noteworthy that each model in the PoM was generated using a unique set of parameters that models a physiological or pathological state (e.g., a low conductance value simulates a conduction block). LHS guarantees that all the parameters are fully represented and, consequently, the PoM comprises of all possible physiological and pathological behaviors of the cellular membrane within the range of variation presented before.

**4.2 Activation–Recovery Intervals Is a Predictive Biomarker.** It was clearly evident that the CO was not capable of predicting the onset of pathology during this experiment. This follows from the abruptness observed in the drop of the CO. The porcine heart was able to maintain a stable output of around 3.8 L/min for over 2 h of experiment, which suddenly ended with a decrease in performance; this phenomenon has been observed in previous PhysioHeart experiments. It should be noted that the reduction in cardiac output, observed at the third time point, would have produced ischemia due to poor coronary perfusion, and together with hyperkalemia it can explain the abrupt ARI shortening observed in Fig. 4(c); but this is only evident at the end of the experiment and it has little predictive value. On the other hand, a strong indication that the condition of the membrane is degrading may be observed in the decreased mode and increased dispersion in the values of the ARIs measured at the second time point, presented in Fig. 4(b); this is important because at this point the CO was still considered normal, so the ARIs can serve as predictive markers of an eventual decrease in cardiac output.

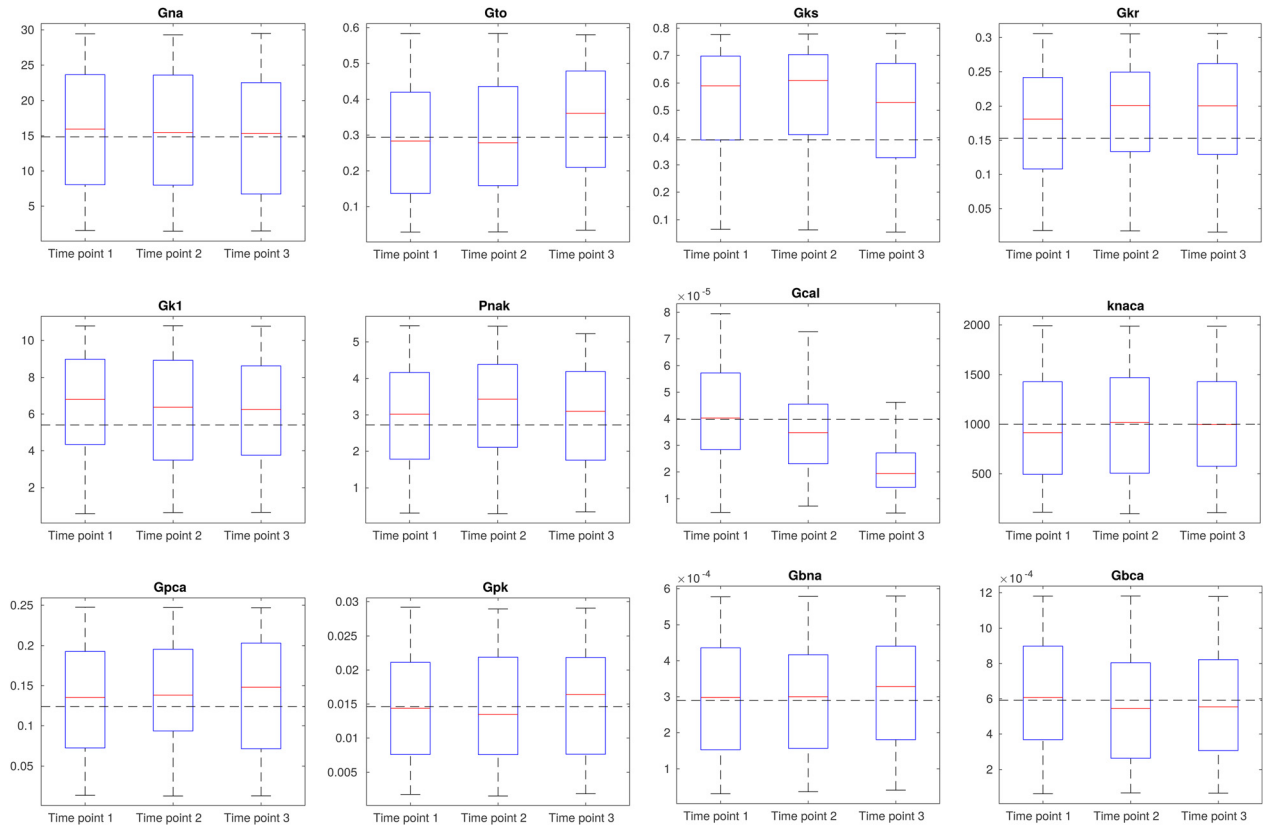


**Fig. 5** Experimentally calibrated populations of models parameter distributions for a representative channel (channel 6) at the three time points. Horizontal dashed lines are the standard values of the parameters from the original TP06 model [14].  $G_x$  are in nS/pF and  $P_{nak}$  and  $k_{naca}$  are in pA/pF.

**4.3 Population of Models Analysis.** Previous studies have shown that APD90 shortening can be a consequence of impaired calcium, potassium, or sodium uptake and release [27]; since the measurement of ion transients is difficult, requiring specialized equipment, a mathematical modeling approach, exemplified by the one implemented here, seems to provide an excellent tool to explore cause-effect relationships and to help elucidating these dynamics, avoiding the need to modify the experimental setup. The results indicate that half of the monitored sites in the membrane were, at time point 2, being affected by a reduction in calcium uptake via L-type channels. This behavior then spread to more sites of the membrane and was accentuated, as can be observed from the results shown for time point 3, and was accompanied by a dramatic reduction in CO. These results appear consistent with those of previous simulations by others [12,27,28], showing that a blockage to L-type calcium current causes APD 90 shortening. Additionally, the L-type channels are one of the main paths by which myocytes obtain calcium, which is needed to activate contraction; hence, an increase in L-type calcium channel resistance could lead to reduction in contractility, which was observed in the experiment. Furthermore, a reduction in L-type calcium conductance would mean that the cells are absorbing less calcium from the environment than in the healthy condition, but the calcium release channels remained unaffected; this would have caused an increase in extracellular calcium; indeed, the experimental measurements showed an increase in ionized calcium concentration in blood.

The ePoM analysis is also sensitive to the constant, although high, potassium concentration in blood, which was around 1.5 times the lower control level (i.e., 5.4 mmol/L). The formulation for the rapid delayed rectifier potassium current, in the TP06 model, is

$$I_{Kr} = G_{Kr} \sqrt{\frac{K_o}{5.4}} x_{r1} x_{r2} (V - E_K) \quad (3)$$

where one can observe that  $I_{Kr}$  is directly proportional to the square root of the external potassium concentration [13]. The observed increase in extra-cellular potassium would affect  $I_{Kr}$  equivalently to multiplying the standard value of  $G_{Kr}$  by 1.22. Indeed, the median value of  $G_{Kr}$  in the ePoM analysis was, as shown in Fig. 5, 1.3 times its standard value. Then, one can potentially conclude that most of the variation in  $G_{Kr}$  can be accounted for by the elevated extracellular potassium concentration, an equivalent analysis can be made for  $I_{K1}$  and  $I_{Ks}$ . Since the three currents were equally affected, the results observed in Fig. 5 are an indication of elevated extracellular potassium concentration.

#### 4.4 Intrasubject Variability in Experimental Acquisitions.

Observe that the boxplots presented in Fig. 5 show that there was an overlap in the values of the ePoM conductances at all times of the experiment; this implies that healthy ion channels can be present at the end point, as well as fully blocked channels during the working mode. This is a typical case of intrasubject variability; a thorough analysis was needed to understand what were the underlying causes of the observed reduction in ARIs. The use of ePoM and their subsequent statistical treatment, explained in this paper, gave the means to distinguish the underlying pathological process (i.e., reduced  $G_{CaL}$  and high extracellular potassium) that was producing the observed reduction in ARI. This predictive effect can be regarded as a consequence of the calibration process, exemplified in Fig. 2, during which many AP morphologies can be fitted to a relatively small range of ARIs; then, the statistical analysis of the ePoMs will only signal a pathological behavior when the

majority of the fitted models contain a value for a conductance that significantly deviates from what is considered healthy.

The method presented in this paper was capable of distinguishing pathology, at an early stage, in an environment where inter and intrasubject variability may have otherwise confused an expert eye. Also, the experimental acquisitions support the ePoM analysis, with the caveat that myocyte contractility and blood samples can only be analyzed after the experiment is over, whereas this ePoM methodology can be applied as soon as the acquisitions are made. Then, the observation of the ARIs provides a means to predict the reduction in cardiac output, and their analysis, through ePoM, is a powerful tool to understand the causes of this reduction during the experiment. This is a significant improvement compared to the methods currently used to monitor these ex vivo experiments [1–3].

**4.5 Versatility of the Experimentally Calibrated Populations of Models Analysis.** The flowchart presented in Fig. 3 also serves to show the modularity of the proposed method. Its different components may be replaced to suit any particular study. For instance, if a particular experiment can perform optical mapping, then the calibration process can be made using several biomarkers, as opposed to a single surrogate, but the process of generating the population remains unchanged. On the other hand, if recent developments produce a more advanced mathematical model, then the PoM can be generated again, but without having to modify the routines that calibrate it to the experimental data. This versatility is a major advantage of the methodology presented in this work.

The use of this method in the analysis of ex vivo experiments could provide the means to enhance our understanding of the cellular causes for chronic cardiac pathologies, like heart failure. Furthermore, this understanding would also provide the tools required to design more effective, patient-specific therapies that target the cellular causes for pathology within individual patients. The use of the method presented in this work to expand limited experimental data is an advancement in the design of minimally invasive diagnostic techniques for the assessment of cardiac pathology.

**4.6 Limitations.** The method presented in this paper as a proof of concept has yielded promising results and it demonstrates a strong approach to the analysis of limited experimental data; it can reach relevant conclusions and minimize the need of computational resources. Nevertheless, there are a number of limitations associated with this approach.

Differences in ion concentrations observed at different times of the experiment were not included when generating the population of models and the vast parameter sampling space ( $15,000^{12}$  possibilities) was not entirely simulated. However, in order to do this, a population of models with *each* of the particular ion concentration combinations and containing all of the parameter combinations (that is  $3 \times 15,000^{12}$  models) should have been generated, which would have rendered this methodology computationally intractable. Nevertheless, the variability captured in the PoM is able to account for the changes in ion concentrations *without* having to generate three sets of populations of models, and Latin hypercube sampling was used since it was designed to capture variability, optimally, in such a large sampling space [18]. Generating and calibrating the PoM as explained in this paper dramatically reduces the number of simulations needed; this approach is supported by various, successful, studies involving populations of cardiac electrophysiology models [12,17,19].

Also, only ARIs were used to assess the electrophysiological state of the heart. While it would have been far more desirable to do optical mapping or transmembrane potential measurements, the technical difficulties of these acquisitions make them incompatible with an implementation in the PhysioHeart platform and impossible to use in patients. On the other hand, epicardial

electrograms can be measured without compromising the experiment and noninvasively in patients, using ECGi [29], which makes ARI an appropriate substitute biomarker. The main challenge in using this single surrogate measurement is that different AP morphologies can result in the same APD90. Intersubject variability is responsible for this, which is why only *statistically significant* differences are regarded as real changes in cellular behavior.

## 5 Conclusions

This paper has presented a novel methodology, based on the statistical analysis of experimentally calibrated populations of models, that can be used to understand the cellular causes for pathological behavior observed in organ-level acquisitions. Notwithstanding its limitations, this proof-of-concept method proved to be a powerful tool to investigate cellular behaviors from organ-level acquisitions. The chief advantage of this ePoM approach is, arguably, the ability to detect pathological behavior while still accounting for inter and intrasubject variability. Another advantage of the proposed method is that it can be seamlessly adapted to the available acquisitions; the population of models only needs to be constructed once and can be calibrated to any, or several, surrogate measurements of action potential biomarkers. This methodology was used to identify the pathological ion dynamics that might have led to the reduced performance of a porcine heart during a PhysioHeart experiment and these were identified before there was an evident reduction in cardiac output; these findings were confirmed by blood samples and contractility analyses made during the same experiment. The use of this statistical approach gave the means to understand the pathological variations that produced reduced cardiac performance during the experiment and it could be used as support in future studies involving drug action. Applying this combined computational and experimental methodology could be an important step forward in the noninvasive assessment of cardiac diseases and in the design of patient-specific therapies to stop the evolution of chronic cardiac maladies.

## Acknowledgment

This project has received funding from the European Union's Horizon 2020 research and innovation program under the Marie Skłodowska-Curie grant agreement No. 642612 under the VPH-CaSE ITN framework<sup>2</sup> and from the Leverhulme Trust through the Senior Research Fellowship "Exploring the Unknowable Using Simulation: Structural Uncertainty in Multiscale Models" (Fellowship No. RF-2015-482).

## Funding Data

- H2020 Marie Skłodowska-Curie Actions (642612).
- Leverhulme Trust (RF-2015-482).

## References

- [1] de Hart, J., de Weger, A., van Tuijl, S., Stijnen, J., van den Broek, C. N., Rutten, M., and de Mol, B. A., 2011, "An Ex Vivo Platform to Simulate Cardiac Physiology: A New Dimension for Therapy Development and Assessment," *Int. J. Artif. Organs*, **34**(6), pp. 495–505.
- [2] Leopaldi, A. M., Vismara, R., van Tuijl, S., Redaelli, A., van de Vosse, F., Fiore, G. B., and Rutten, M., 2015, "A Novel Passive Left Heart Platform for Device Testing and Research," *Med. Eng. Phys.*, **37**(4), pp. 361–366.
- [3] Tuzun, E., Pennings, K., van Tuijl, S., de Hart, J., Stijnen, M., van de Vosse, F., de Mol, B., and Rutten, M., 2014, "Assessment of Aortic Valve Pressure Overload and Leaflet Functions in an Ex Vivo Beating Heart Loaded With a Continuous Flow Cardiac Assist Device," *Eur. J. Cardio-Thorac. Surg.*, **45**(2), pp. 377–383.
- [4] Boukens, B. J., and Efimov, I. R., 2014, "A Century of Optocardiography," *IEEE Rev. Biomed. Eng.*, **7**, pp. 115–125.

<sup>2</sup><http://vph-case.eu>

- [5] Gima, K., and Rudy, Y., 2002, "Ionic Current Basis of Electrocardiographic Waveforms a Model Study," *Circ. Res.*, **90**(8), pp. 889–896.
- [6] Dutta, S., Mincholé, A., Quinn, T. A., and Rodriguez, B., 2017, "Electrophysiological Properties of Computational Human Ventricular Cell Action Potential Models Under Acute Ischemic Conditions," *Prog. Biophys. Mol. Biol.*, **129**, pp. 40–52.
- [7] Yamashita, Y., 1982, "Theoretical Studies on the Inverse Problem in Electrocardiography and the Uniqueness of the Solution," *IEEE Trans. Biomed. Eng.*, **29**(11), pp. 719–725.
- [8] Gemmell, P., Burrage, K., Rodríguez, B., and Quinn, T. A., 2016, "Rabbit-Specific Computational Modelling of Ventricular Cell Electrophysiology: Using Populations of Models to Explore Variability in the Response to Ischemia," *Prog. Biophys. Mol. Biol.*, **121**(2), pp. 169–184.
- [9] Britton, O. J., Bueno-Orovio, A., Van Ammel, K., Lu, H. R., Towart, R., Gallacher, D. J., and Rodríguez, B., 2013, "Experimentally Calibrated Population of Models Predicts and Explains Intersubject Variability in Cardiac Cellular Electrophysiology," *Proc. Natl. Acad. Sci.*, **110**(23), pp. E2098–E2105.
- [10] Muszkiewicz, A., Bueno-Orovio, A., Liu, X., Casadei, B., and Rodriguez, B., 2014, "Constructing Human Atrial Electrophysiological Models Mimicking a Patient-Specific Cell Group," *Computing in Cardiology Conference (CinC)*, Cambridge, MA, Sept. 7–10, pp. 761–764.
- [11] Sánchez, C., Bueno-Orovio, A., Wettwer, E., Loose, S., Simon, J., Ravens, U., Pueyo, E., and Rodríguez, B., 2014, "Inter-Subject Variability in Human Atrial Action Potential in Sinus Rhythm Versus Chronic Atrial Fibrillation," *PLoS One*, **9**(8), p. e105897.
- [12] Zhou, X., Bueno-Orovio, A., Orini, M., Hanson, B., Hayward, M., Taggart, P., Lambiase, P. D., Burrage, K., and Rodriguez, B., 2016, "In Vivo and in Silico Investigation Into Mechanisms of Frequency Dependence of Repolarization Alternans in Human Ventricular Cardiomyocytes," *Circ. Res.*, **118**(2), pp. 266–278.
- [13] Ten Tusscher, K., Noble, D., Noble, P., and Panfilov, A., 2004, "A Model for Human Ventricular Tissue," *Am. J. Physiol. Heart Circ. Physiol.*, **286**(4), pp. H1573–H1589.
- [14] Ten Tusscher, K. H., and Panfilov, A. V., 2006, "Alternans and Spiral Breakup in a Human Ventricular Tissue Model," *Am. J. Physiol. Heart Circ. Physiol.*, **291**(3), pp. H1088–H1100.
- [15] Zile, M. A., and Trayanova, N. A., 2015, "Rate-Dependent Force, Intracellular Calcium, and Action Potential Voltage Alternans Are Modulated by Sarcomere Length and Heart Failure Induced-Remodeling of Thin Filament Regulation in Human Heart Failure: A Myocyte Modeling Study," *Prog. Biophys. Mol. Biol.*, **120**(1–3), pp. 270–280.
- [16] Weise, L. D., and Panfilov, A. V., 2013, "A Discrete Electromechanical Model for Human Cardiac Tissue: Effects of Stretch-Activated Currents and Stretch Conditions on Restitution Properties and Spiral Wave Dynamics," *PLoS One*, **8**(3), p. e59317.
- [17] Dutta, A. M. S., Walmsley, J., and Rodriguez, B., 2013, "Ionic Mechanisms of Variability in Electrophysiological Properties in Ischemia: A Population-Based Study," *Computing in Cardiology Conference (CinC)*, Zaragoza, Spain, Sept. 22–25, pp. 691–694.
- [18] McKay, M. D., Beckman, R. J., and Conover, W. J., 2000, "A Comparison of Three Methods for Selecting Values of Input Variables in the Analysis of Output From a Computer Code," *Technometrics*, **42**(1), pp. 55–61.
- [19] Muszkiewicz, A., Britton, O. J., Gemmell, P., Passini, E., Sánchez, C., Zhou, X., Carusi, A., Quinn, T. A., Burrage, K., Bueno-Orovio, A., and Rodriguez, B., 2016, "Variability in Cardiac Electrophysiology: Using Experimentally-Calibrated Populations of Models to Move Beyond the Single Virtual Physiological Human Paradigm," *Prog. Biophys. Mol. Biol.*, **120**(1–3), pp. 115–127.
- [20] Coronel, R., de Bakker, J. M., Wilms-Schopman, F. J., Opthof, T., Linnenbank, A. C., Belterman, C. N., and Janse, M. J., 2006, "Monophasic Action Potentials and Activation Recovery Intervals as Measures of Ventricular Action Potential Duration: Experimental Evidence to Resolve Some Controversies," *Heart Rhythm*, **3**(9), pp. 1043–1050.
- [21] Haws, C. W., and Lux, R. L., 1990, "Correlation Between In Vivo Transmembrane Action Potential Durations and Activation-Recovery Intervals From Electrograms. Effects of Interventions That Alter Repolarization Time," *Circulation*, **81**(1), pp. 281–288.
- [22] Potse, M., Vinet, A., Opthof, T., and Coronel, R., 2009, "Validation of a Simple Model for the Morphology of the T Wave in Unipolar Electrograms," *Am. J. Physiol. Heart Circ. Physiol.*, **297**(2), pp. H792–H801.
- [23] Mann, H. B., and Whitney, D. R., 1947, "On a Test of Whether One of Two Random Variables Is Stochastically Larger Than the Other," *Ann. Math. Stat.*, **18**(1), pp. 50–60.
- [24] Bowman, T. A., and Hughes, H. C., 1984, "Swine as an In Vivo Model for Electrophysiologic Evaluation of Cardiac Pacing Parameters," *Pacing Clin. Electrophysiology*, **7**(2), pp. 187–194.
- [25] Laursen, M., Olesen, S.-P., Grunnet, M., Mow, T., and Jespersen, T., 2011, "Characterization of Cardiac Repolarization in the Göttingen Minipig," *J. Pharmacol. Toxicol. Methods*, **63**(2), pp. 186–195.
- [26] Arlock, P., Mow, T., Sjöberg, T., Arner, A., Steen, S., and Laursen, M., 2017, "Ion Currents of Cardiomyocytes in Different Regions of the Göttingen Minipig Heart," *J. Pharmacol. Toxicol. Methods*, **86**, pp. 12–18.
- [27] Mahajan, A., Sato, D., Shiferaw, Y., Baher, A., Xie, L.-H., Peralta, R., Olcese, R., Garfinkel, A., Qu, Z., and Weiss, J. N., 2008, "Modifying L-Type Calcium Current Kinetics: Consequences for Cardiac Excitation and Arrhythmia Dynamics," *Biophys. J.*, **94**(2), pp. 411–423.
- [28] Zenzemi, N., and Rodriguez, B., 2015, "Effects of L-Type Calcium Channel and Human Ether-a-Go-Go Related Gene Blockers on the Electrical Activity of the Human Heart: A Simulation Study," *Europace*, **17**(2), pp. 326–333.
- [29] Ghanem, R. N., Jia, P., Ramanathan, C., Ryu, K., Markowitz, A., and Rudy, Y., 2005, "Noninvasive Electrocardiographic Imaging (ECGI): Comparison to Intraoperative Mapping in Patients," *Heart Rhythm*, **2**(4), pp. 339–354.